ACS OMEGA

http://pubs.acs.org/journal/acsodf

Article

Structural Properties and Hopping Conduction in the Normal State of Electron-Doped Superconductor Cuprate $Eu_{2-x}Ce_xCuO_{4+\alpha-\delta}$

Yati Maryati,* Suci Winarsih, Muhammad Abdan Syakuur, Maykel Manawan, Togar Saragi,* and Risdiana*

Cite This: *ACS Omega* 2022, 7, 12601−12609

Read Online

ACCESS | Metrics & More | Article Recommendations

ABSTRACT: Electron-doped superconducting cuprate of $Eu_{2-x}Ce_xCuO_{4+\alpha-\delta}$ has been studied in the whole doping regime from x = 0.10−0.20 with reducing oxygen content to investigate the relation between the crystal structure and the hopping conduction in the normal state. Parameter of the crystal structure has been extracted from the X-ray diffraction (XRD) measurement while hopping conduction parameters have been obtained from resistivity measurements. The Eu−O bond length decreases with the increasing doping concentration, indicating the successful doping by the partial replacing of Eu^{3+} with Ce^{4+}. The resistivity increases with decreasing temperature in all measured samples. This is an indication of bad metal-like behavior in the whole regime in the normal state of electron-doped superconducting cuprate of $Eu_{2-x}Ce_xCuO_{4+\alpha-\delta}$. The temperature dependence of resistivity was analyzed by the Arrhenius law and the variable range hopping model. It is found that the hopping conduction mechanism more likely follows the variable range hopping rather than the Arrhenius law, indicating that the hopping mechanism occurs in three dimensions. The Cu−O bond length probably plays an important role in decreasing the activation energy. The decreasing value of the activation energy correlates with the increase in the localization radius.

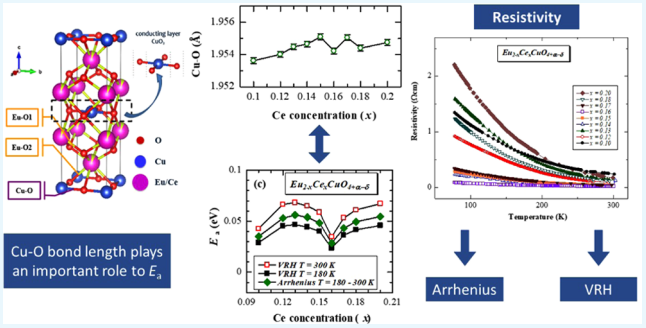

INTRODUCTION

Understanding the phase diagram of high-T_c superconducting cuprate (HTSC) has attracted huge attention since its first discovery, and it is still an open discussion. The superconductivity emerges when both hole and electron charge carriers are doped into the mother compound of antiferromagnetic Mott insulator.[1,2] It is believed that the superconductivity of HTSC appears under a strong influence of spin correlations of the Mott insulator in the mother compound.[2−7] Physical properties of superconductors derived from mother compounds have been extensively investigated in the past few decades. However, some physical properties in the normal states related to the origin of the superconducting are still not clear. In the case of a hole-doped superconducting cuprate of $La_{2-x}Sr_xCuO_4$, it is reported that a strange metal with resistivity linearly proportional to temperature (T) is observed in the normal state in the near-optimal doping regime around x = 0.15, which is very different from the conventional metal whose resistivity is directly proportional to T^2.[8,9] The strange metal behavior in the normal state is thought to be linked to the quantum critical point (QCP), indicating a change in the nature of the ground state at x around 0.19.[7−10] It is suggested that the linear dependence of resistivity and temperature also occurs in the electron-doped superconducting cuprate.[9] This means that it is more important to study the physical properties of the normal state to understand the origin of superconductivity, a critical question in the HTSC system. However, the reports explaining the temperature dependence of resistivity in the normal state of electron-doped superconducting cuprate are very few. In this study, we report the temperature dependence of resistivity on the electron-doped superconducting cuprate $Eu_{2-x}Ce_xCuO_{4+\alpha-\delta}$.

The relationship between electrical properties and superconductivity can be studied by analyzing the mobility of electrons due to the effect of doping concentration, x, and oxygen content. In our previous study, it was found that $Eu_{2-x}Ce_xCuO_{4+\alpha-\delta}$ exhibited a bad metal when x = 0.09, 0.15, and 0.16 in the normal state, indicating an increase in resistivity.[11,12] Here, we expand the Ce concentration of $Eu_{2-x}Ce_xCuO_{4+\alpha-\delta}$ from an underdoped regime to an overdoped regime to study the electrical properties in the normal

Received: November 3, 2021
Accepted: March 21, 2022
Published: April 5, 2022

state. The Arrhenius law and Mott's variable range hopping (VRH) model were used for analyzing the carrier transport mechanism.[13−15] We aim to compare these two models to get a better understanding of the hopping conduction mechanism.

In addition to the transport properties and superconductivity, it is also very important to study the crystalline structure. The polycrystalline electron-doped $Eu_{2-x}Ce_xCuO_{4+\alpha-\delta}$ has a tetragonal T' structure with a planar configuration of CuO_2 plane as the conducting layer[16] and (Eu,Ce)−O as the charge reservoir. Generally, superconductivity can be determined by the presence of a cooper pair in the conduction layer, which comes from the charge reservoir. In the case of a Fe−As-based superconductor $LaO_{1-x}F_xFeAs$, the lattice parameters and the atomic bond lengths are related to the T_c value. It was reported that the bond length of La−As is inversely proportional to the value of T_c.[17] Although the relationship between bond length and physical properties such as T_c has been reported in FeAs-based superconductors, such reports on other types of superconductors have not been completely clarified. One such report is about the relationship between the bond length and physical properties of a superconducting cuprate system. In this report, the relationship between the structure and transport properties of $Eu_{2-x}Ce_xCuO_{4+\alpha-\delta}$ is given.

EXPERIMENT

Powder samples of the electron-doped superconducting cuprate of $Eu_{2-x}Ce_xCuO_{4+\alpha-\delta}$ were prepared by a solid-state reaction method.[11,16,18] The concentration of Ce (x) was set in the range between x = 0.10 and 0.20. All powder precursors of Eu_2O_3, CeO_2, and CuO were weighed in certain stoichiometric ratios, pulverized, and prefired at 900 °C for 20 h. All of the prefired samples were reground and pressed into pellets with a diameter of 10 mm and then sintered at 1050 °C for 16 h. The samples obtained were referred to as-grown samples of $Eu_{2-x}Ce_xCuO_{4+\alpha}$, where α is the excess oxygen in the sample and is estimated to have a value much less than 1 ($|\alpha| \ll 1$).[18] Furthermore, to reduce the excess oxygen (α), the as-grown samples were annealed in an argon gas flow at various temperatures in the range of 900−930 °C for 10 to 20 h.[11−13,16,19,20] The value of δ was obtained from the weight change before and after the annealing process. It was found that the δ value was in the range of 0.011−0.097 as shown in Table 1.

The crystal structure and quality of all samples were measured at room temperature by powder X-ray diffraction (XRD) with Cu Kα using a D8 Advance Bruker machine. The range of XRD measurement is 2θ = 20−70°. The phase purity, weighted R profile (R_{wp}), goodness of fit (GoF), lattice parameter, and bond length of $Eu_{2-x}Ce_xCuO_{4+\alpha-\delta}$ were analyzed by the Rietveld refinement method. The value of R_{wp} and GoF could explain the suitability and quality of the sample compared to the reference. The resistivity of the samples was carried out using the four-point probe method in the temperature range of 78−300 K.

Table 1. $Eu_{2-x}Ce_xCuO_{4+\alpha-\delta}$ Samples with Various x and δ Values

x	δ
0.10	0.082
0.12	0.029
0.13	0.022
0.14	0.038
0.15	0.044
0.16	0.011
0.17	0.097
0.18	0.026
0.20	0.068

RESULTS AND DISCUSSION

The XRD patterns of the polycrystalline $Eu_{2-x}Ce_xCuO_{4+\alpha-\delta}$ with concentrations of x = 0.10, 0.12, 0.13, 0.14, and 0.15 are shown in Figure 1a−e, respectively, and those with x = 0.16, 0.17, 0.18, and 0.20 are shown in Figure 1f−i, respectively. The XRD pattern of another electron-doped sample $Pr_{0.86}LaCe_{0.14}CuO_4$ (PLCCO) with a T' structure is also displayed for reference in Figure 1j. The major peaks of all samples correspond to the T' tetragonal structure with a space group of I4/mmm of the $Eu_{2-x}Ce_xCuO_{4+\alpha-\delta}$ phase. The impurity peaks at x = 0.14, 0.16, 0.17, 0.18, and 0.20 were identified as CeO_2 peaks, which might affect its transport properties.

Figure 2 shows that the crystal structure of $Eu_{2-x}Ce_xCuO_{4+\alpha-\delta}$ consists of a conducting layer of CuO_2 plane and a charge reservoir of (Eu,Ce)−O. The Cu−O bond is in the conducting layer area, while Eu−O1 and Eu−O2 bonds are located in the charge reservoir.

Table 2 summarizes the phase purity, weighted R profile (R_{wp}), goodness of fit (GoF), lattice parameters (a-axis, c-axis), unit cell volume, and the bond lengths of Eu−O and Cu−O. The phase purity for this sample is in the range of 95.4−100%, while the R_{wp} and GoF values are in the range of 6.6325−12.6880 and 0.8754−1.6390, respectively. The average values of phase purity, R_{wp}, and GoF are 98.24%, 8.6826, and 1.1739 respectively, indicating that the samples were of high quality. The lattice parameters obtained are in the range of 3.9072−3.9102 Å for the a-axis and 11.8444−11.8712 Å for the c-axis. These values are in good agreement with the values of 3.9080 and 11.8410 Å of the parameters of the a-axis and c-axis, respectively, as reported for $Eu_{1.85}Ce_{0.15}CuO_4$.[21] Compared with those of its mother compound Eu_2CuO_4, the a-axis values of $Eu_{2-x}Ce_xCuO_{4+\alpha-\delta}$ are greater and the c-axis values of $Eu_{2-x}Ce_xCuO_{4+\alpha-\delta}$ are smaller. For Eu_2CuO_4, the value of the lattice parameter of the a-axis value is 3.9047 Å and that of the c-axis is 11.9126 Å.[22] The lattice parameters of the c-axis tend to decrease due to the partial replacement of Eu^{3+} by Ce^{4+}, which has a smaller ionic radius than Eu^{3+}. The decrease in the values of the lattice parameters of the c-axis leads to a decrease in the unit cell volume.

The Eu−O1 bond length is in the range of 2.2915−2.2925 Å and Eu−O2 is in the range of 2.6333−2.6354 Å. In the case of the mother compound Eu_2CuO_4, the values of Eu−O1 and Eu−O2 bond lengths are 2.3215 and 2.6623 Å, respectively.[23] It is found that the Eu−O1 and Eu−O2 bond lengths are significantly decreased due to Ce doping substitution in the Eu site.

The Cu−O bond lengths of $Eu_{2-x}Ce_xCuO_{4+\alpha-\delta}$ are in the range of 1.9536−1.9551 Å. The Cu−O bond length increases with the increase in the Ce doping concentration and suddenly drops at x = 0.16, as shown in Figure 3. This phenomenon is probably related to the transport properties, which are discussed in the next section.

Figure 4 shows the temperature dependence of resistivity of $Eu_{2-x}Ce_xCuO_{4+\alpha-\delta}$. The resistivity increases with the decrease in temperature to 78 K. This indicates that the normal state of $Eu_{2-x}Ce_xCuO_{4+\alpha-\delta}$ has bad metal-like behavior. The bad metal-like behavior in this study is most likely because the sample is still in a polycrystalline form and not a single-crystal form. It has been

https://doi.org/10.1021/acsomega.1c06161
ACS Omega 2022, 7, 12601−12609

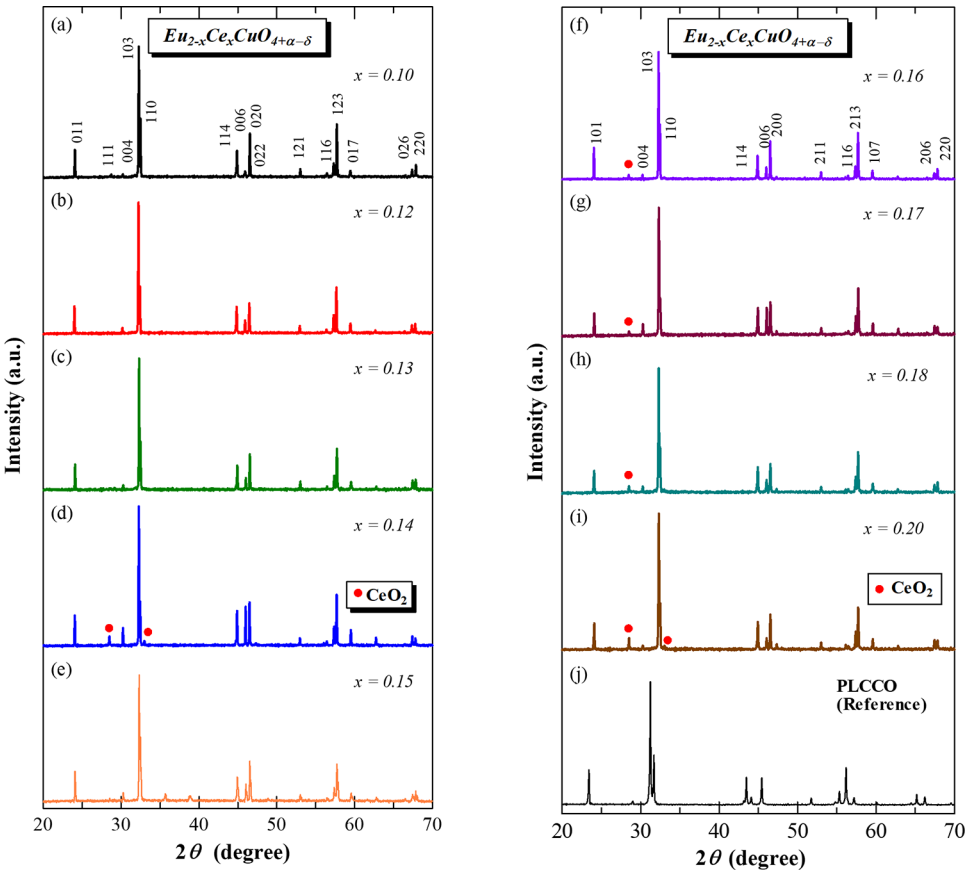

Figure 1. XRD patterns of $Eu_{2-x}Ce_xCuO_{4+\alpha-\delta}$ with $x = 0.10$ (a), 0.12 (b), 0.13 (c), 0.14 (d), 0.15 (e), 0.16 (f), 0.17 (g), 0.18 (h), and 0.20 (i) and the reference sample of PLCCO (j).

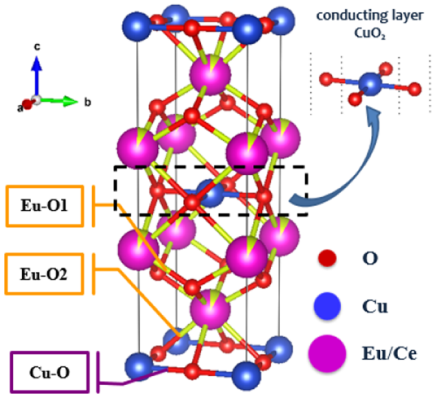

Figure 2. Crystal structure of $Eu_{2-x}Ce_xCuO_{4+\alpha-\delta}$.

reported that for single crystals, the resistivity shows a metal-like behavior in the normal state at temperatures above T_c;[24] therefore, the bad metal-like behavior in this report is only found in samples in the polycrystalline form.

The bad metal-like behavior in the normal state of $Eu_{2-x}Ce_xCuO_{4+\alpha-\delta}$ is due to the presence of localized charges. The origin of the localized charges can be understood by analyzing the temperature dependence of resistivity using the Arrhenius law and the variable range hopping (VRH) model.[13,15] The Arrhenius law is shown in eq 1.

$$\sigma = \sigma_o \exp\left(\frac{-E_a}{k_B T}\right) \quad (1)$$

where σ is the conductivity of the sample ($\sigma = \frac{1}{\rho}$, where ρ is the resistivity of the sample), σ_o is the constant conductivity of the pre-exponential factor, T is the absolute temperature, E_a is the activation energy, and k_B is the Boltzmann constant. In this model, the hopping mechanism of the charge carriers occurs in the nearest neighboring sites. Hence, the hopping range and the activation energy are temperature independent.[13,15] Figure 5a shows the temperature dependence of resistivity (on the logarithmic scale) of $Eu_{2-x}Ce_xCuO_{4+\alpha-\delta}$ in the temperature range of 78−300 K. Resistivity as an inverse function of temperature, $1/T$, is presented in Figure 5b−d to estimate the value of activation energy in the temperature ranges 78−110, 110−180, and 180−300 K, respectively. It is clearly observed that the resistivity of all samples decreases as temperature increases.

Figure 6a−c shows that the values of activation energy tend to increase with the increase in Ce doping concentrations in the range of 0.59×10^{-2}−0.69×10^{-2} eV for the temperature range of 78−110 K, 1.37×10^{-2}−2.20×10^{-2} eV for the temperature range of 110−180 K, and 2.86×10^{-2}−5.61×10^{-2} eV for the temperature range of 180−300 K. The complete values of the activation energy for various Ce contents using the Arrhenius law are listed in Table 3.

The interesting point is that the E_a value at $x = 0.16$ shows the smallest value of activation energy along with $x = 0.10$ in all temperature ranges. The smallest activation energy indicates that it is easier for the charge carrier to hop from its localization area. The smallest E_a value observed at $x = 0.16$ requires further investigation whether it is related to QCP as is the case for

https://doi.org/10.1021/acsomega.1c06161
ACS Omega 2022, 7, 12601−12609

Table 2. Phase Purity, Weighted R profile (R_{wp}), Goodness of Fit (GoF), Lattice Parameters, and Bond Length of $Eu_{2-x}Ce_xCuO_{4+\alpha-\delta}$

				lattice parameter (Å)			bond length (Å)		
x	phase purity (%)	R_{wp}	GoF	a	c	V (Å^3)	Eu−O1	Eu−O2	Cu−O
0.10	100	7.5930	1.0637	3.9072	11.8712	181.2321	2.2922	2.6354	1.9536
0.12	100	8.0216	1.2488	3.9080	11.8560	181.0729	2.2917	2.6342	1.9540
0.13	100	8.5301	0.8754	3.9089	11.8544	181.1342	2.2921	2.6344	1.9545
0.14	95.4	9.3300	1.6390	3.9093	11.8511	181.1157	2.2920	2.6341	1.9547
0.15	100	12.6880	1.1541	3.9102	11.8529	181.1395	2.2925	2.6347	1.9551
0.16	97.6	7.7134	1.2147	3.9084	11.8509	181.0332	2.2925	2.6338	1.9542
0.17	97.1	8.4317	1.0052	3.9101	11.8449	181.0905	2.2920	2.6338	1.9551
0.18	96.1	6.6325	1.0818	3.9088	11.8444	180.9632	2.2915	2.6333	1.9544
0.20	98.0	9.2029	1.2828	3.9095	11.8468	181.0694	2.2919	2.6338	1.9548

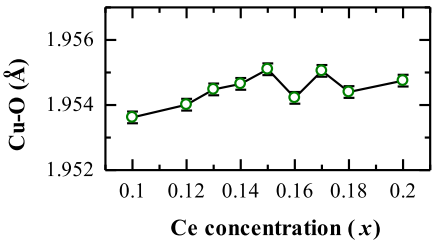

Figure 3. Cerium doping concentration dependence of the Cu−O bond length in $Eu_{2-x}Ce_xCuO_{4+\alpha-\delta}$.

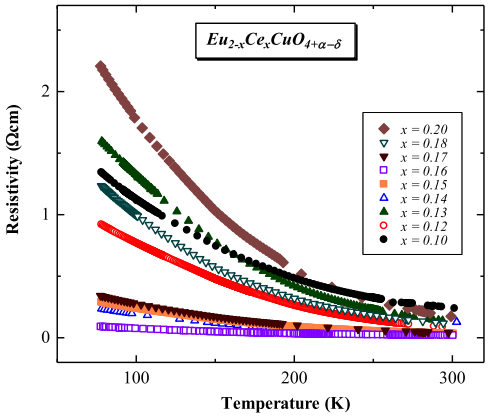

Figure 4. Temperature dependence of resistivity of $Eu_{2-x}Ce_xCuO_{4+\alpha-\delta}$.

$Pr_{1-x}Ce_xCuO_4$ (PCCO).[25] For PCCO samples, the resistivity followed the behavior of T^{β}, with the smallest exponential value of β occurring at the doping concentration $x = 0.165$. Therefore, for PCCO material, $x = 0.165$ is a quantum critical point that separates two regions with different physical properties in their ground state, namely, Fermi liquid state and non-Fermi liquid state.[25] Therefore, the investigation of the QCP phenomena in ECCO becomes an important research topic to be carried out in the future.

Since the mother compound of electron-doped superconducting cuprate behaves like a Mott insulator, we also analyze the hopping conduction mechanism of $Eu_{2-x}Ce_xCuO_{4+\alpha-\delta}$ using Mott's VRH model. This model explains that the hopping range and the activation energy depend on temperature so that the hopping mechanism occurs not only with the nearest neighboring sites but also with other sites that are very different from the Arrhenius law. The superconductivity and electronic state of electron-doped superconducting cuprate are strongly dependent on the hopping conduction mechanism. For this purpose, we analyze the hopping conduction mechanism of $Eu_{2-x}Ce_xCuO_{4+\alpha-\delta}$ using the VRH model described in eq 2.

$$\sigma = \sigma_0 \exp\left[-\left(\frac{T_0}{T}\right)^p\right] \tag{2}$$

where σ is the conductivity of the sample, σ_0 is the constant conductivity, and p is the hopping dimension ($p = \frac{1}{n+1}$, where n is hopping direction). For instance, if the hopping direction is in three dimensions, the value of p is 1/4 and T_0 is the characteristic temperature constant that can be obtained using eq 3.

$$T_0 = \left[\frac{24}{\pi r^3 k_B N(E_F)}\right] \tag{3}$$

where r is the localization radius, $N(E_F)$ is the density of states of electrons at the Fermi level, and k_B is the Boltzmann constant. The activation energy of charge carriers can be estimated by eq 4.

$$E_a = p k_B (T_0)^p T^{1-p} \tag{4}$$

Figure 7 depicts ln ρ as a function of $T^{-1/4}$, showing a linear relation between resistivity and $T^{-1/4}$ for each range of temperature. It is indicated that the hopping mechanism might occur in three dimensions with $p = 1/4$ instead of the nearest neighboring sites only.

The value of E_a obtained from eq 4 with $p = 1/4$ is in the range of 0.52×10^{-2}−0.79×10^{-2} eV for temperature range of 78−110 K, 0.52×10^{-2}−2.49×10^{-2} eV for the temperature range of 110−180 K, and 2.37×10^{-2} −6.73×10^{-2} eV for the temperature of 180−300 K, as shown in Figure 8a−c, respectively.

The values of the activation energy obtained from the Arrhenius law are between the values of E_a at the highest and the lowest temperatures obtained from the VRH model, as shown in Figure 9. A similar result was also found in another Mott insulator compound of $BaTiO_3$.[13] It is also reported that the value of E_a from VRH better explains the hopping conduction mechanism in a Mott insulator than that from the Arrhenius law. Additionally, both models give the same tendency in the activation energy as a function of the Ce doping concentration.

In addition to the activation energy, the value of T_0 can be obtained from the gradient value in Figure 7. The value of T_0 can also be elucidated using eq 5.

https://doi.org/10.1021/acsomega.1c06161
ACS Omega 2022, 7, 12601−12609

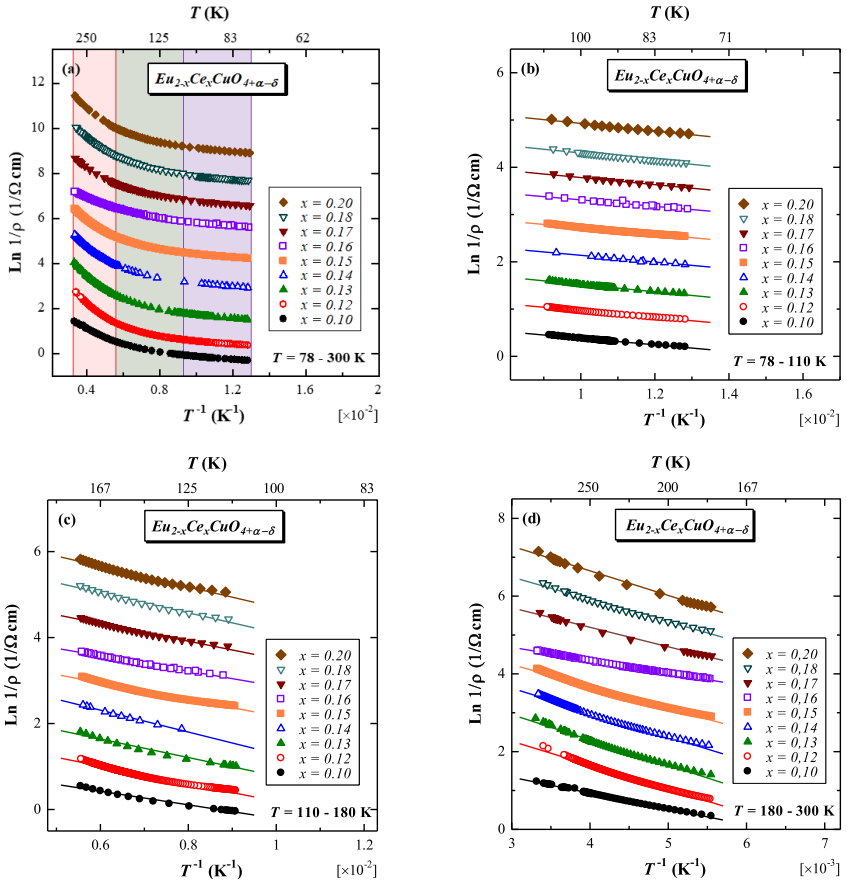

Figure 5. Temperature dependence of resistivity (on a logarithmic scale) of $Eu_{2-x}Ce_xCuO_{4+\alpha-\delta}$ in the temperature ranges 78−300 K (a), 78−110 K (b), 110−180 K (c), and 180−300 K (d).

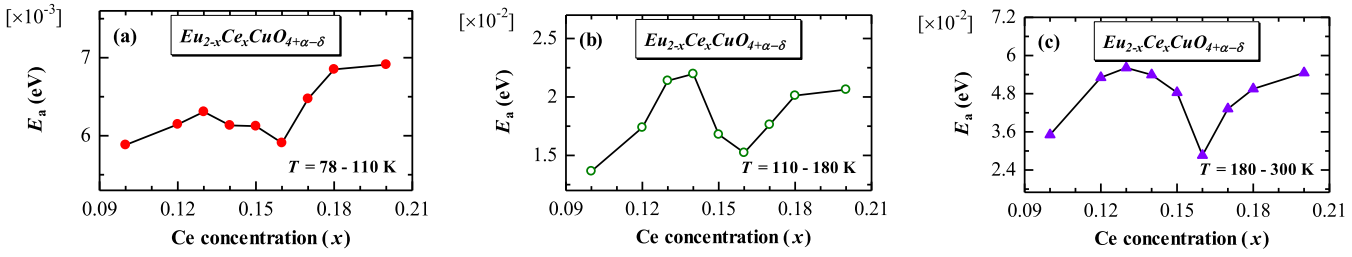

Figure 6. Activation energy of $Eu_{2-x}Ce_xCuO_{4+\alpha-\delta}$ obtained by applying the Arrhenius law to the resistivity data in the temperature range between 78−110 K (a), 110−180 K (b), and 180−300 K (c).

Table 3. Value of the Activation Energy (E_a) for $Eu_{2-x}Ce_xCuO_{4+\alpha-\delta}$

	E_a ($\times 10^{-2}$ eV)		
Ce (x)	78−110 K	110−180 K	180−300 K
0.10	0.59	1.37	3.51
0.12	0.62	1.74	5.31
0.13	0.63	2.14	5.61
0.14	0.61	2.20	5.39
0.15	0.61	1.68	4.84
0.16	0.59	1.52	2.86
0.17	0.65	1.76	4.32
0.18	0.69	2.01	4.95
0.20	0.69	2.06	5.46

$$T_0 = \frac{\gamma}{k_B g(\mu) r^3} \tag{5}$$

The value of T_0 depends on the density level in the region near the Fermi energy ($g(\mu)$), the localization radius near the Fermi energy level (r), and the numerical coefficient (γ). By assuming $\frac{\gamma}{k_B g(\mu)}$ to be constant c, the value of r can be obtained, as shown in eq 6.

$$r \sim \sqrt[3]{c\frac{1}{T_0}} \tag{6}$$

Figure 10 shows the Ce (x) concentration dependence of localization radius (r). The value of r is in the range of 4.10×10^{-2}−5.16×10^{-2} Å for the temperature range 78−110 K, 1.46×10^{-2}−7.62×10^{-2} Å for the temperature range 110−180 K, and 0.64×10^{-2}−1.59×10^{-2} Å for the temperature range 180−300 K, as shown in Figure 10a−c, respectively. The localization radius decreases gradually with the increase in the doping concentration up to x = 0.14. Then, the localization radius

https://doi.org/10.1021/acsomega.1c06161
ACS Omega 2022, 7, 12601−12609

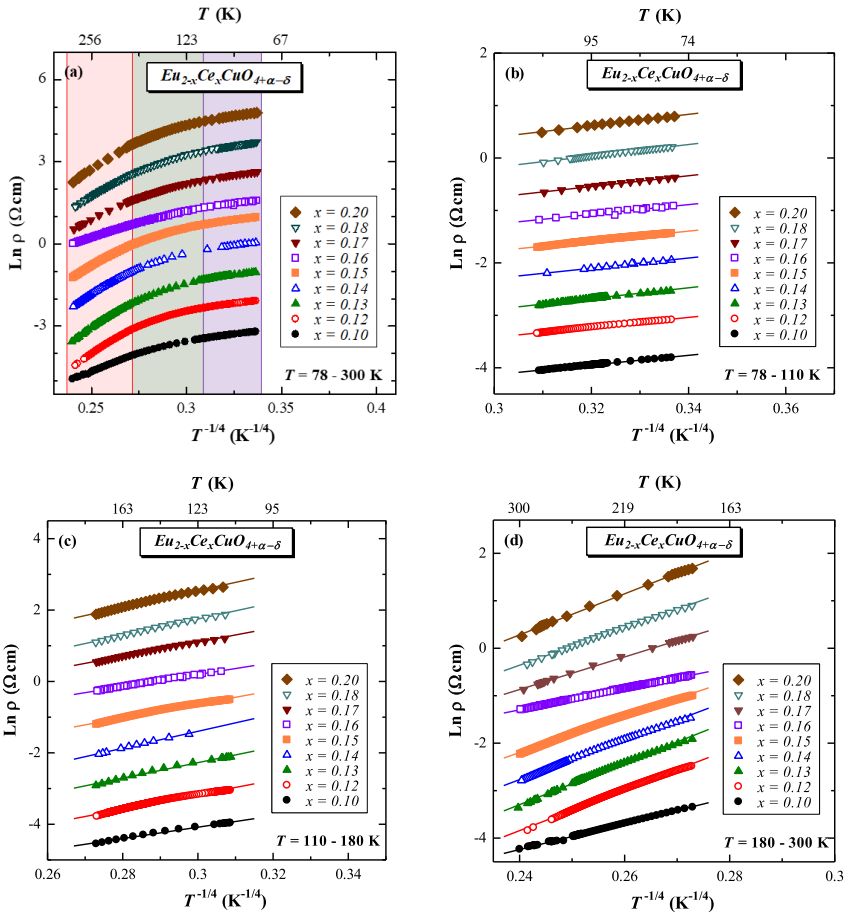

Figure 7. Dependence of ln ρ on $T^{-1/4}$ in $Eu_{2-x}Ce_xCuO_{4+\alpha-\delta}$ in the temperature ranges of 78−300 K (a), 78−110 K (b), 110−180 K (c), and 180−300 K (d).

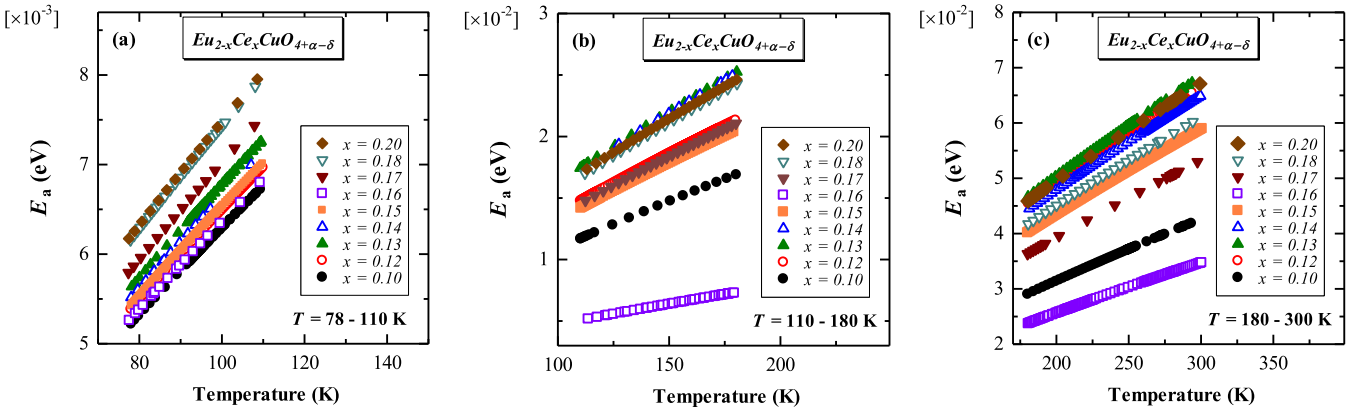

Figure 8. Activation energy of $Eu_{2-x}Ce_xCuO_{4+\alpha-\delta}$ using the variable range hopping model in the temperature ranges of 78−110 K (a), 110−180 K (b), and 180−300 K (c).

increases with the increase in doping concentration at $x = 0.15-0.16$ near optimum doping concentration and decreases in an overdoped concentration. It can be clearly observed that the value of r at $x = 0.16$ is the largest compared to other concentrations. As the localization radius increases, the required energy for the mobility of the charge carriers becomes smaller.

The results of the analysis of the Cu−O bond length (as shown in Figure 3), E_a value (as shown in Figures 6 and 9), and r (as shown in Figure 10) for the ECCO sample with $x = 0.16$ are very interesting to discuss. The E_a value at $x = 0.16$ obtained from the Arrhenius law is 0.59×10^{-2} eV for the temperature range 78−110 K, 1.52×10^{-2} eV for the temperature range 110−180 K, and 2.86×10^{-2} eV for the temperature range 180−300 K. From the VRH model, the smallest average value of E_a is 0.58×10^{-3} eV for the temperature range 78−110 K, 0.71×10^{-3} eV for the temperature range 110−180 K, and 2.9×10^{-3} eV for the temperature range 180−300 K, as shown in Figures 6 and 9, respectively. The highest r value at $x = 0.16$ is 5.08×10^{-2} Å for the temperature range 78−110 K, 7.62×10^{-2} Å for the temperature range 110−180 K, and 1.59×10^{-2} Å for the temperature range 180−300 K. Also, the small value of the Cu−O bond length at $x = 0.16$ is 1.9542 Å. A sudden decrease in the

https://doi.org/10.1021/acsomega.1c06161
ACS Omega 2022, 7, 12601−12609

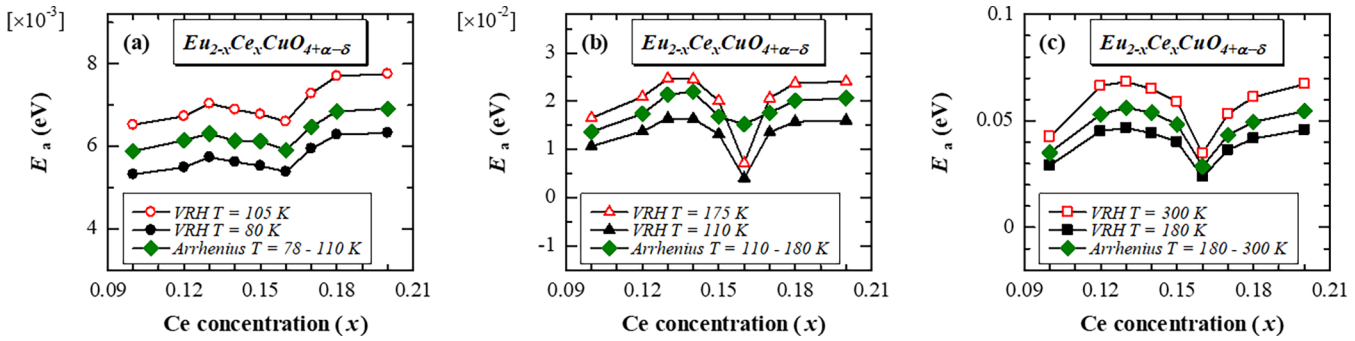

Figure 9. Activation energy of $Eu_{2-x}Ce_xCuO_{4+\alpha-\delta}$ obtained by applying the Arrhenius law and the variable range hopping model to the resistivity data in the temperature ranges of 78−110 K (a), 110−180 K (b), and 180−300 K (c).

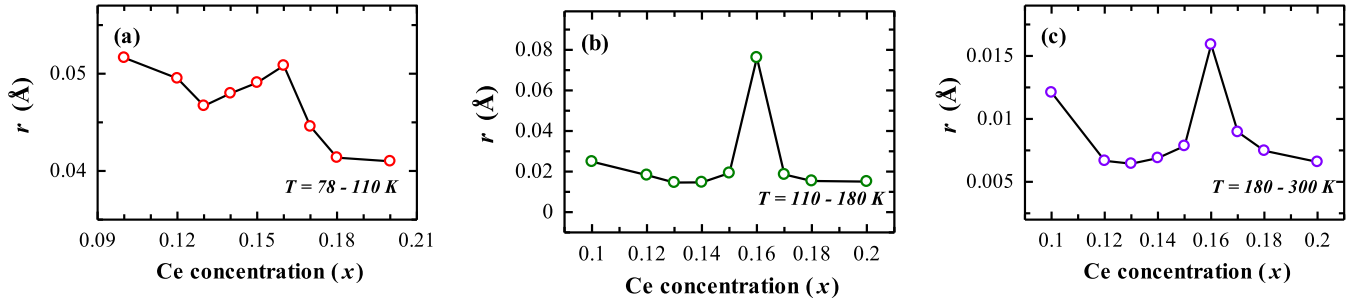

Figure 10. Ce (x) concentration dependence of localization radius (r) in the temperature ranges of 78−110 K (a), 110−180 K (b), and 180−300 K (c).

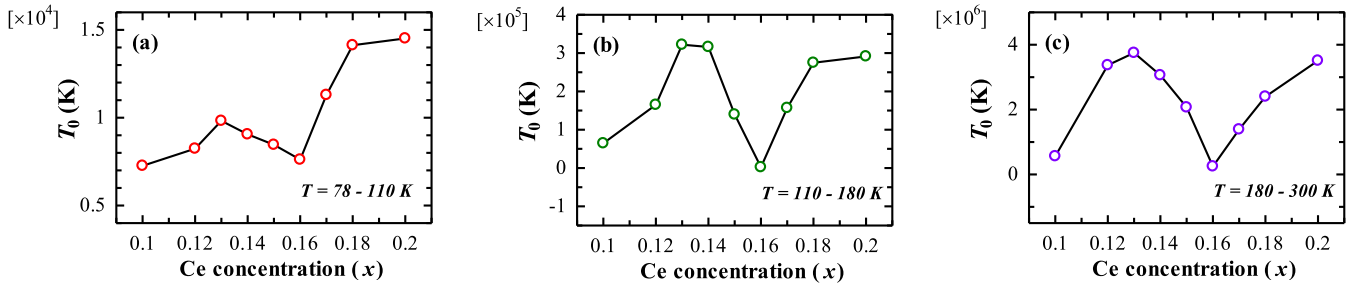

Figure 11. Ce (x) concentration dependence of characteristic temperature (T_o) in the temperature ranges 78−110 K (a), 110−180 K (b), and 180−300 K (c).

Cu−O bond length probably causes a decrease in the value of the activation energy, which indicates the energy required for the charge carriers to move or leave the localization area. The decrease in the value of E_a correlates with the increase in the localization radius. This is in accordance with Figures 6 and 9, which show E_a has the smallest value at x = 0.16. However, further studies are needed to understand the relation between the short bond length of Cu−O and the decrease in E_a.

The value of T_0 is in the range of 0.73×10^4−1.45×10^4 K for the temperature range 78−110 K, 0.02×10^5−3.22×10^5 K for the temperature range 110−180 K, and 0.25×10^6−3.75×10^6 K for the temperature range 180−300 K, as shown in Figure 11a−c, respectively. The results of T_0 in the temperature range 180−300 K are in accordance with those reported by Birgeneau et al. in single-crystal La_2CuO_4 (LCO),[26] where the value of T_0 is in the range of 2×10^6−6×10^6 K. The value of T_0 is a parameter that describes the Coulombic repulsion energy, so the similar value of T_0 between ECCO and LCO at high temperatures indicates that the value of the Coulombic repulsion energy is also similar to each other.

CONCLUSIONS

The crystalline structure and transport properties of $Eu_{2-x}Ce_xCuO_{4+\alpha-\delta}$ with x = 0.10−0.20 have been studied. XRD measurement analysis shows that all samples have major peaks that correspond to the T' tetragonal structure. Samples with x = 0.10, 0.12, 0.13, and 0.15 have 100% phase purity, while those with x = 0.14, 0.16, 0.17, 0.18, and 0.20 still have small amount of impurity peaks related to CeO_2. The values of lattice constants are in good agreement with those reported in the reference. Compared with that of its mother compound Eu_2CuO_4, the values of lattice parameters of the c-axis tend to decrease due to the partial replacement of Eu^{3+} by Ce^{4+}, which has a smaller ionic radius than that of Eu^{3+}. This is also supported by the significantly reduced Eu−O bond length due to Ce doping substitution in the Eu site.

The resistivity increases with the decrease in temperature to 78 K, indicating that $Eu_{2-x}Ce_xCuO_{4+\alpha-\delta}$ has bad metal-like behavior in the normal state because the samples are in polycrystalline form. The conduction mechanism in $Eu_{2-x}Ce_xCuO_{4+\alpha-\delta}$ follows the variable range hopping rather

https://doi.org/10.1021/acsomega.1c06161
ACS Omega 2022, 7, 12601−12609

than the Arrhenius law, indicating that the hopping mechanism occurs in three dimensions instead of the nearest neighboring sites only. The activation energy is inversely proportional to the localization radius, which is assumed due to the sudden decrease in the Cu−O bond length at $x = 0.16$. There may be a correlation between the Cu−O bond length and the activation energy that affects the localization radius. Further studies on the relation between the short bond length, conduction mechanism, and QCP are needed.

AUTHOR INFORMATION

Corresponding Authors

Yati Maryati − *Department of Physics, Faculty of Mathematics and Natural Sciences, Universitas Padjadjaran, Sumedang 45363 West Java, Indonesia;* orcid.org/0000-0002-8510-9990; Email: yati.maryati@unpad.ac.id

Togar Saragi − *Department of Physics, Faculty of Mathematics and Natural Sciences, Universitas Padjadjaran, Sumedang 45363 West Java, Indonesia*; Email: t.saragi@phys.unpad.ac.id

Risdiana − *Department of Physics, Faculty of Mathematics and Natural Sciences, Universitas Padjadjaran, Sumedang 45363 West Java, Indonesia*; Phone: +62 (0)22 7797712; Email: risdiana@phys.unpad.ac.id; Fax: +62 (0)22 7794545

Authors

Suci Winarsih − *Department of Physics, Faculty of Mathematics and Natural Sciences, Universitas Padjadjaran, Sumedang 45363 West Java, Indonesia;* orcid.org/0000-0001-8457-7410

Muhammad Abdan Syakuur − *Department of Physics, Faculty of Mathematics and Natural Sciences, Universitas Padjadjaran, Sumedang 45363 West Java, Indonesia*

Maykel Manawan − *Faculty of Defense Technology, Indonesia Defense University, Bogor 16810 West Java, Indonesia*

Complete contact information is available at: https://pubs.acs.org/10.1021/acsomega.1c06161

Notes

The authors declare no competing financial interest.

ACKNOWLEDGMENTS

The authors would like to thank Kemenristek-DIKTI of the Republic of Indonesia for financial support for the research in the scheme of Fundamental Research (Penelitian Dasar Unggulan Perguruan Tinggi) 2021, Contract No. 1207/UN6.3.1/PT.00/2021. This work was also partially supported by the Academic Leadership Grant (ALG) of Universitas Padjadjaran 2021, No. 1959/UN6.3.1/PT.00/2021. SW would also like to thank Universitas Padjadjaran for Post-Doctoral Research Grant No. 3570/UN6.3.3/LT/2020. In addition, the authors would also like to thank Y. Koike, M. Kato, T. Noji, and T. Kawamata from the Department of Applied Physics, Tohoku University, Japan, for their support in the XRD and resistivity measurements.

REFERENCES

(1) Armitage, N. P.; Fournier, P.; Greene, R. L. Progress and Perspectives on Electron-doped Cuprates. *Rev. Mod. Phys.* **2010**, *82*, 2421−2487.

(2) Keimer, B.; Kivelson, S. A.; Norman, M. R.; Uchida, S.; Zaanen, J. From Quantum Matter to High-Temperature Superconductivity in Copper Oxides. *Nature* **2015**, *518*, 179−186.

(3) Budnick, J. I.; Chamberland, B.; Yang, D. P.; Niedermayer, C.; Golnik, A.; Recknagel, E.; Rossmanith, M.; Weidinger, A. Dependence of the Nèel-Temperatures of La_2CuO_4 on Sr-Doping Studied by Muon Spin Rotation. *Europhys. Lett.* **1988**, *5*, 651−656.

(4) Saylor, J.; Tacaks, L.; Hohenemser, C.; Budnick, J. I.; Chamberland, B. Néel Temperature of Stoichiometric La_2CuO_4. *Phys. Rev. B* **1989**, *40*, 6854−6861.

(5) Croft, T. P.; Lester, C.; Senn, M. S.; Bombardi, A.; Hayden, S. M. Charge Density Wave Fluctuations in $La_{2-x}Sr_xCuO_4$ and Their Competition with Superconductivity. *Phys. Rev. B: Condens. Matter Mater. Phys.* **2014**, *89*, No. 224513.

(6) Hitti, B.; Birrer, P.; Fischer, K.; Gygax, F. N.; Lippelt, E.; Maletta, H.; Schenck, A.; Weber, M. Study of La_2CuO_4 and Related Compounds by μSR. *Hyperfine Interact.* **1991**, *63*, 287−294.

(7) Sarkar, T.; Mandal, P. R.; Poniatowski, N. R.; Chan, M. K.; Greene, R. L. Correlation Between Scale-Invariant Normal-State Resistivity and Superconductivity in an Electron-doped Cuprate. *Sci. Adv.* **2019**, *5*, No. eaav6753.

(8) Sachdev, S. Where is The Quantum Critical Point in The Cuprate Superconductors? *Phys. Status Solidi B* **2010**, *247*, 537−543.

(9) Legros, A.; Benhabib, S.; Tabis, W.; Laliberté, F.; Dion, M.; Lizaire, M.; Vignolle, B.; Vignolles, D.; Raffy, H.; Li, Z. Z.; Auban-Senzier, P.; DOIron-Leyraud, N.; Fournier, P.; Colson, D.; Taillefer, L.; Proust, C. Universal T-Linear Resistivity and Planckian Dissipation in Overdoped Cuprates. *Nat. Phys.* **2019**, *15*, 142−147.

(10) Galanakis, D.; Khatami, E.; Mikelsons, K.; MacRidin, A.; Moreno, J.; Browne, D. A.; Jarrell, M. Quantum Criticality and Incipient Phase Separation in the Thermodynamic Properties of The Hubbard Model. *Philos. Trans. R. Soc., A* **2011**, *369*, 1670−1686.

(11) Maryati, Y.; Hanifah, A. I.; Subardhi, M. A. B.; Rahayu, E. A.; Tayubi, Y. R.; Manawan, M.; Saragi, T.; Risdiana. The Effect of Heating Treatment in Electron Doped Superconductor Eu1.85Ce0.15-CuO4+α-δ. *J. Phys.: Conf. Ser.* **2018**, *1080*, No. 012022.

(12) Tayubi, Y. R.; Maryati, Y.; Nafisah, N.; Aulia, D. G.; Nurwati, E.; Amalia, T.; Syakuur, M. A.; Wiendartun; Feranie, S.; Saragi, T.; Risdiana. Study of Purity and Electrical Resistivity of Eu1.91Ce0.09-CuO4 and Eu1.84Ce0.16CuO4. *Key Eng. Mater.* **2020**, *860*, 160−164.

(13) Han, H.; Davis, C.; Nino, J. C. Variable Range Hopping Conduction in $BaTiO_3$ Ceramics Exhibiting Colossal Permittivity. *J. Phys. Chem. C* **2014**, *118*, 9137−9142.

(14) Rathod, S. G.; Bhajantri, R. F.; Ravindrachary, V.; Pujari, P. K.; Nagaraja, G. K.; Naik, J.; Hebbar, V.; Chandrappa, H. Temperature-Dependent Ionic Conductivity and Transport Properties of $LiClO_4$-doped PVA/Modified Cellulose Composites. *Bull. Mater. Sci.* **2015**, *38*, 1213−1221.

(15) Winarsih, S.; Budiman, F.; Tanaka, H.; Adachi, T.; et al. Variable Range Hopping Resistivity in $La_{2-x}Sr_xCuO_4$ Nanoparticles Evaluated by Four Point Probe Method. *Key Eng. Mater.* **2020**, *860*, 142−147.

(16) Risdiana Manawan, M.; Safriani, L.; Saragi, T.; Somantri, W. A.; Aprilia, A.; Syakir, N.; Hidayat, S.; Bahtiar, A.; Fitrilawati; Siregar, R. E. Study of Transport and Magnetic Properties of Electron-Doped Superconducting Cuprates Eu1.85Ce0.15Cu1-yZnyO4+α-δ. *Phys. C* **2019**, *557*, 41−43.

(17) Chen, N.; Yang, L.; YaKui, J.; ShaoPeng, Q.; WanJie, Z.; Yang, L. Effect of Bond Length and Radius on Superconducting Transition Temperature for FeAs-Based Superconductors. *Sci. China: Phys., Mech. Astron.* **2010**, *53*, 59−63.

(18) Risdiana, R.; Adachi, T.; Oki, N.; Koike, Y.; Suzuki, T.; Watanabe, I. Muon Spin Relaxation Study of The Cu Spin Dynamics in Electron-Doped High- Tc Superconductor Pr0.86LaCe0.14Cu1-yZnyO4. *Phys. Rev. B: Condens. Matter Mater. Phys.* **2010**, *82*, No. 014506.

(19) Charikova, T. B.; Shelushinina, N. G.; Harus, G. I.; Petukhov, D. S.; Petukhova, O. E.; Ivanov, A. A. Resistivity Tensor Correlations in the Mixed State of Electron-Doped Superconductor $Nd_{2-x}Ce_xCuO_{4+\delta}$. *Phys. C* **2016**, *525*−*526*, 78−83.

(20) Yamamoto, M.; Kohori, Y.; Fukazawa, H.; Takahashi, A.; Ohgi, T.; Adachi, T.; Koike, Y. Existence of Large Antiferromagnetic Spin Fluctuations in Ce-Doped T′-Cuprate Superconductors. *J. Phys. Soc. Jpn* **2016**, *85*, No. 024708.
(21) Niwa, K.; Kamehara, N.; Uzumaki, T. Crystal Structure and Madelung Potential in R2-xCexCuO4- $_{\delta}$ (R=Pr, Nd, Sm, Eu and Gd) System. *Jpn. J. Appl. Phys.* **1991**, *30*, L981−L984.
(22) Fujita, M.; Suzuki, K. M.; Asano, S.; Okabe, H.; Koda, A.; Kadono, R.; Watanabe, I. Magnetic Behavior of T -type Eu_2CuO_4 Revealed by Muon Spin Rotation and Relaxation Measurements. *Phys. Rev. B* **2020**, *102*, No. 045116.
(23) dataset The Materials Project Materials Data on Eu2CuO4 by Materials Project. https://materialsproject.org/materials/mp-22306/ (accessed May 14, 2021).
(24) Krockenberger, Y.; Kurian, J.; Naito, M.; Alff, L. Epitaxial Growth of Superconducting $Eu_{2-x}Ce_xCuO_4$ Thin Films. *Jpn. J. Appl. Phys.* **2008**, *47*, 6307.
(25) Dagan, Y.; Qazilbash, M. M.; Hill, C. P.; Kulkarni, V. N.; Greene, R. L. Evidence for a Quantum Phase Transition in $Pr_{2-x}Ce_xCuO_{4-\delta}$ from Transport Measurements. *Phys. Rev. Lett.* **2004**, *92*, No. 167001.
(26) Birgeneau, R. J.; Chen, C. Y.; Gabbe, D. R.; Jensen, H. P.; Kastner, M. A.; Peters, C. J.; Picone, P. J.; Thio, T.; Thurston, T. R.; Tuller, H. L.; et al. Soft-Phonon Behavior and Transport in Single-Crystal La_2CuO_4. *Phys. Rev. Lett.* **1987**, *59*, 1329−1332.

https://doi.org/10.1021/acsomega.1c06161
ACS Omega 2022, 7, 12601−12609